

Quantifying the effects of nutrient enrichment and freshwater mixing on coastal ocean acidification



Key Points:

- Eutrophication is a strong driver of coastal acidification in Buzzards Bay
- Aragonite undersaturation was observed in the most impacted embayments
- A quantitative framework is presented to determine the improvements to coastal acidification under nutrient loading reduction scenarios

Supporting Information:

- Supporting Information Data S1

Correspondence to:

J. E. Rheuban,
jrheuban@whoi.edu

Citation:

Rheuban, J. E., Doney, S. C., McCorkle, D. C., & Jakuba, R. W. (2019). Quantifying the effects of nutrient enrichment and freshwater mixing on coastal ocean acidification. *Journal of Geophysical Research: Oceans*, 124. <https://doi.org/10.1029/2019JC015556>

Received 9 AUG 2019

Accepted 1 OCT 2019

Accepted article online 7 NOV 2019

Jennie E. Rheuban¹ , Scott C. Doney^{1,2} , Daniel C. McCorkle³, and Rachel W. Jakuba⁴

¹Department of Marine Chemistry and Geochemistry, Woods Hole Oceanographic Institution, Woods Hole, MA, USA, ²Department of Environmental Sciences, University of Virginia, Charlottesville, VA, USA, ³Department of Geology and Geophysics, Woods Hole Oceanographic Institution, Woods Hole, MA, USA, ⁴Buzzards Bay Coalition, New Bedford, MA, USA

Abstract The U.S. Northeast is vulnerable to ocean and coastal acidification because of low alkalinity freshwater discharge that naturally acidifies the region, and high anthropogenic nutrient loads that lead to eutrophication in many estuaries. This study describes a combined nutrient and carbonate chemistry monitoring program in five embayments of Buzzards Bay, Massachusetts to quantify the effects of nutrient loading and freshwater discharge on aragonite saturation state (Ω). Monitoring occurred monthly from June 2015 to September 2017 with higher frequency at two embayments (Quissett and West Falmouth Harbors) and across nitrogen loading and freshwater discharge gradients. The more eutrophic stations experienced seasonal aragonite undersaturation, and at one site, nearly every measurement collected was undersaturated. We present an analytical framework to decompose variability in aragonite Ω into components driven by temperature, salinity, freshwater endmember mixing, and biogeochemical processes. We observed strong correlations between apparent oxygen utilization and the portion of aragonite Ω variation that we attribute to biogeochemistry. The regression slopes were consistent with Redfield ratios of dissolved inorganic carbon and total alkalinity to dissolved oxygen. Total nitrogen and the contribution of biogeochemical processes to aragonite Ω were highly correlated, and this relationship was used to estimate the likely effects of nitrogen loading improvements on aragonite Ω . Under nitrogen loading reduction scenarios, aragonite Ω in the most eutrophic estuaries could be raised by nearly 0.6 units, potentially increasing several stations above the critical threshold of 1. This analysis provides a quantitative framework for incorporating ocean and coastal acidification impacts into regulatory and management discussions.

1. Introduction

Over the past decade, ocean acidification has emerged as a major concern and negative consequence of rising atmospheric carbon dioxide (Doney, Balch, et al., 2009). Ocean acidification has been shown to significantly affect marine calcifiers, both experimentally and under natural field conditions (Barton et al., 2012; Kroeker et al., 2013, 2014; Waldbusser & Salisbury, 2014). Marine calcifiers are particularly sensitive to ocean acidification's effects on calcium carbonate (CaCO_3) mineral saturation state (Ω), which is a measure of the thermodynamic stability of CaCO_3 . Increased carbon dioxide invasion in the surface ocean is projected to cause significant declines in global ocean pH and Ω by the end of the century (Feely et al., 2009; Doney, Balch, et al., 2009; Bopp et al., 2013).

Open-ocean acidification, driven by atmospheric carbon dioxide trends, is relatively well constrained for surface waters under future climate scenarios. However, projecting changes in nearshore environments is much more complicated because coastal ecosystems are affected by a number of additional processes such as freshwater discharge, eutrophication, and upwelling (Alin et al., 2012; Cai et al., 2011; Wallace et al., 2014). Given that many coastal economies rely heavily on calcifying species sensitive to ocean acidification, the future impact of ocean and coastal acidification is likely to affect coastal communities disproportionately. For instance, significant social vulnerability and economic losses are projected in the future for coastal communities that rely on shellfish as a food source or for economic revenue (Cooley et al., 2012; Cooley et al., 2015; Cooley & Doney, 2009; Ekstrom et al., 2015; Mathis et al., 2015). The U.S. Northeast has been identified as particularly vulnerable both socially due to regional dependence on sensitive fisheries (Ekstrom et al., 2015; Hare et al., 2016) and environmentally because nearshore seawater buffering capacity is already limited due

©2019. The Authors.

This is an open access article under the terms of the Creative Commons Attribution License, which permits use, distribution and reproduction in any medium, provided the original work is properly cited.

to low-alkalinity source water (Gledhill et al., 2015; Wang et al., 2013; Wanninkhof et al., 2015). This region is also severely impacted by eutrophication due to increasing coastal development (Valiela et al., 1997, 2016; Williamson et al., 2017) and thus is vulnerable to periodic or chronic low pH and Ω (Ekstrom et al., 2015; Wallace et al., 2014). Some estuaries and nearshore ecosystems already experience seasonal aragonite saturation states that approach or are below 1 (Wallace et al., 2014; Gledhill et al., 2015; Wang et al., 2017), indicating environments that may be particularly stressful to calcifiers.

The eutrophication problem in the U.S. Northeast is widespread and is both ecologically and economically damaging (Liu et al., 2017; Merrill et al., 2018; Nicholls & Crompton, 2018). Many coastal embayments in the U.S. Northeast have been designated impaired as pertaining to section 303(d) of the Clean Water Act (Massachusetts Department of Environmental Protection (MassDEP) 2017; Cape Cod Commission, 2017). Impaired coastal waters require the development of total maximum daily load (TMDL) limits to address and mitigate the negative effects of nutrient pollution and improve water quality. TMDL development requires observational studies combined with hydrodynamic and water quality modeling efforts to quantify target nutrient concentrations throughout the water body based on current and possible future nitrogen loading scenarios (e.g., Howes et al., 2006, 2012, 2013, 2014, 2015). To reach these TMDL limits and resulting improved nitrogen concentrations, communities develop water quality management plans that specifically target and reduce eutrophication through nitrogen loading reduction strategies (e.g., Cape Cod 208 plan, Cape Cod Commission, 2015, 2017). These management plans include provisions related to the impacts of nitrogen or phosphorous pollution but do not currently consider improvements to coastal acidification as a potential benefit to nutrient remediation. From a management perspective, addressing eutrophication-driven coastal acidification through a regulatory framework using the Clean Water Act could benefit from direct quantification of the degree of impact of nutrient pollution on Ω (Sakashita, 2016).

Here, we describe a combined water quality and carbonate chemistry monitoring program designed to characterize the seasonal and multi-year variations in carbonate and nutrient chemistry across nitrogen loading and freshwater discharge gradients in Buzzards Bay, Massachusetts (MA). We provide an analytical framework that can be used to quantify the impacts of eutrophication on Ω and other inorganic carbon system metrics such as pH, and using the observed relationships between monitored eutrophication indicators and Ω , we project possible improvements and increases in Ω as a consequence of reductions in nitrogen loading under future loading scenarios.

2. Methods

2.1. Site Description

Buzzards Bay, MA is a shallow, elongated basin of approximately 11 m mean depth that is the location of an intensive, long-term citizen-science water quality monitoring program run by the Buzzards Bay Coalition, a nonprofit organization whose mission is to protect and restore the health of Buzzards Bay. This monitoring program has documented strong declines in Buzzards Bay's water quality over the past several decades that may be related to nutrient loads or to regional warming (Rheuban et al., 2016; Williamson et al., 2017).

The coastline of Buzzards Bay includes many small embayments with distinct watersheds that all receive tidal inflow from Buzzards Bay, yet have dramatically different water quality due to differences in land use and development, geomorphology, hydrodynamics, and watershed-to-estuary ratios. Land use within each embayment's watershed ranges from urban and heavily developed (e.g., New Bedford Harbor) to agriculturally dominated (e.g., Westport River) to mixed forests with sparse housing developments (e.g., Quissett Harbor; Williamson et al., 2017). In this work, we collaborated with the Buzzards Bay Coalition to augment their existing nutrient monitoring program by adding carbonate chemistry measurements.

2.2. Sample Collection and Processing

Of the approximately 200 stations regularly monitored by the Buzzards Bay Coalition, 10 stations in five embayments and a station in the open waters of Buzzards Bay were chosen for additional carbonate chemistry monitoring (Figure 1). We selected stations with the longest nutrient monitoring history, which represented endmembers in freshwater inputs and underlying nitrogen loads and water quality. All five embayments sampled also have technical reports that determine their nitrogen loads through the

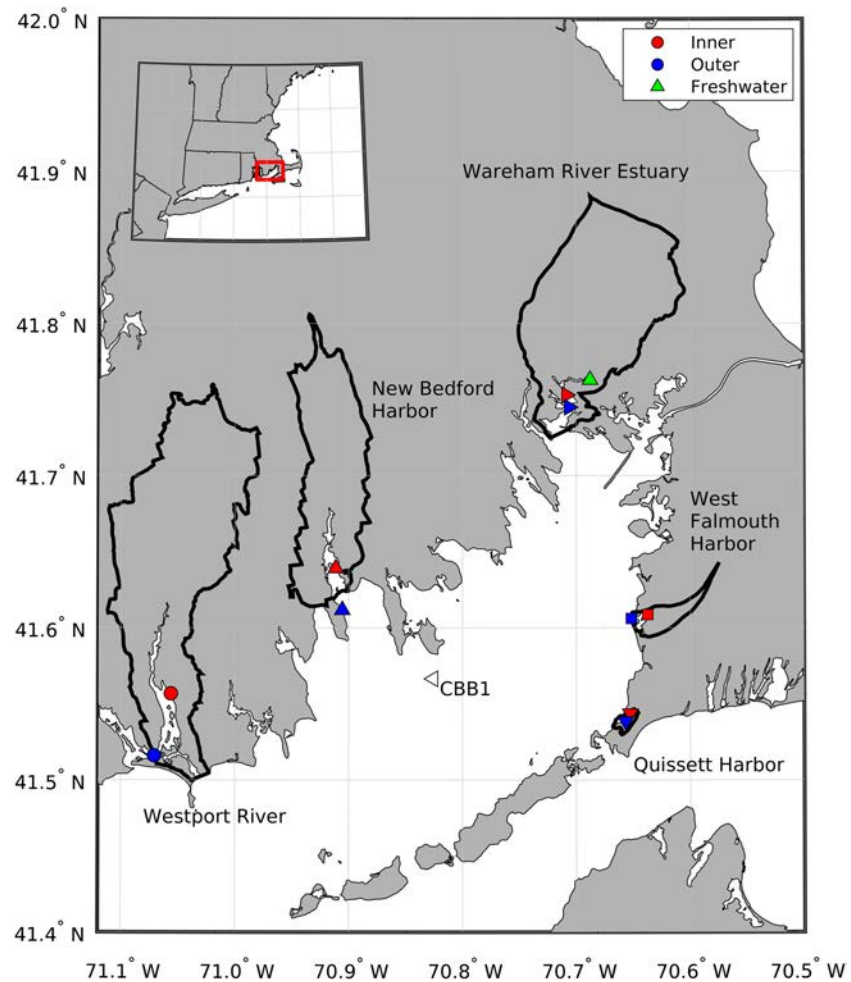


Figure 1. Map of sampling stations. Blue stations are designated “outer harbors,” red stations are designated “inner harbors,” the open triangle is the reference Buzzards Bay station CBB1, and the green triangle is the location of the freshwater endmember sample collection. Unique symbols are given to distinguish individual embayments that remain consistent in figures throughout the manuscript. Names and watersheds for each of the embayments are also included.

Table 1
Estimated Nitrogen Load Normalized by Estuary Volume for the Five Harbors Studied in This Analysis

| Harbor | Nitrogen load | TN | Salinity |
|----------------------------|--|-------------------|----------|
| | ($\text{kg N m}^{-3} \text{ yr}^{-1}$) | (μM) | (PSU) |
| New Bedford Harbor | 7.37 | 55.5 | 27.6 |
| Quissett Harbor | 1.10 | 23.6 | 31.0 |
| Wareham River Estuary | 9.49 | 39.6 | 22.8 |
| West Falmouth Harbor | 14.3 | 37.0 | 28.0 |
| Westport River—East Branch | 14.4 | 55.2 | 24.6 |

Note. Total nitrogen (TN) concentration is the 1992–2013 spatio-temporal embayment average concentration collected in July and August by the Buzzards Bay Coalition. Data are from Rheuban et al. (2016) and Williamson et al. (2017). Nitrogen loads are estimated from Howes et al. (2006, 2012, 2013, 2014, 2015).

Massachusetts Estuaries Project (MEP, Howes et al., 2006, 2012, 2013, 2014, 2015), which uses data and sampling stations from the Buzzards Bay Coalition as validation for their nitrogen load estimates and modeling efforts.

Each embayment contained two sampling stations, denoted as “inner” or “outer,” that reflected within-embayment nutrient and/or salinity gradients due to freshwater inputs, residence time, or enhanced localized nitrogen inputs. Freshwater inputs in the east branch of the Westport River (hereafter, Westport), New Bedford Harbor (hereafter, New Bedford), and the Wareham River Estuary (hereafter, Wareham) were dominated by surface waters, while West Falmouth Harbor (hereafter West Falmouth) and Quissett Harbor (hereafter, Quissett) were dominated by groundwater inputs. Estimates of nitrogen loading rates, normalized by estuary volume, varied across embayments (Table 1). Freshwater samples were also collected during July 2017 in the nontidal portion of the upper Agawam River that feeds into the Wareham River estuary complex.

Bottle samples for carbonate and nutrient chemistry were collected at least monthly at all nearshore stations from June 2015 to May 2017, and sampling in Quissett and West Falmouth continued through September 2017. The station located in the open waters of Buzzards Bay was not sampled from February to April 2017 because of logistical constraints. During the June–September period, samples were collected every other week at Quissett and West Falmouth stations. In concert with the Buzzards Bay Coalition's monitoring protocols and EPA-approved Quality Assurance Project Plan (Williams & Neill, 2014), samples were collected during the last 3 hours of an outgoing tide, generally during ebb tides that occurred in the morning. Samples were collected from 0.5 to 1 m depth for carbonate chemistry and 0.15 m for nutrient chemistry. With the exception of CBB1, stations were <3 m deep at low tide.

Two-hundred fifty milliliter bottle samples for carbonate chemistry were fixed with 100 μl of a saturated HgCl_2 solution immediately upon collection to inhibit biological activity. Samples were processed for dissolved inorganic carbon (DIC) and total alkalinity (ALK) on a Marianda VINDTA 3C. DIC was measured using coulometric titration, and ALK was measured with open cell Gran titration; both analyses were standardized using a seawater Certified Reference Material obtained from A. Dickson at Scripps Institution of Oceanography. Several duplicate bottles were processed from each sampling day to ensure consistency and achieved an average standard deviation across duplicate bottles of $\pm 5.8 \mu\text{mol kg}^{-1}$ for DIC and $\pm 1.1 \mu\text{mol kg}^{-1}$ for ALK. Separate bottle samples were also analyzed for nutrient chemistry, including $\text{NO}_2^- + \text{NO}_3^-$, NH_4^+ , PO_4^{3-} , dissolved organic nitrogen, particulate organic nitrogen, particulate organic carbon, chlorophyll a, and phaeophytin. Methodologies of nutrient analyses are given in Williams and Neill (2014) and Rheuban et al. (2016). Nutrient samples were processed either at the Marine Biological Laboratory or the Woods Hole Oceanographic Institution Nutrient Facility. Ancillary site characteristics (temperature, salinity, and dissolved oxygen) were measured with YSI85, YSIProPlus, or YSI600XL handheld meters calibrated prior to sampling. The full carbonate system was calculated using CO2SYS for Matlab (Lewis & Wallace 1998) using the K1 and K2 dissociation coefficients from Millero et al. (2010) and KSO_4 dissociation coefficients from Dickson (1990) with total borate from Uppstrom (1974). Apparent oxygen utilization (AOU) was calculated from dissolved oxygen measurements as the difference between saturation oxygen concentration at in situ temperature and salinity and observed oxygen concentration. Total nitrogen (TN) concentration under different loading scenarios was obtained from the MEP reports for each embayment (Howes et al., 2006, 2012, 2013, 2014, 2015).

2.3. Data Analysis

Calcium carbonate mineral saturation state, Ω , is defined using the product of calcium and carbonate ion concentrations:

$$\Omega = [\text{Ca}^{2+}][\text{CO}_3^{2-}]/K_{\text{sp}}, \quad (1)$$

where K_{sp} is the effective thermodynamic solubility product. In this analysis, we focus on Ω with respect to the carbonate mineral aragonite, since all bivalves produce an initial shell made of aragonite, and many also produce aragonite shells as adults. Hereafter, when referring to Ω , we refer to aragonite saturation state. We investigated the factors driving regional and seasonal variations in Ω computed from temperature (T), salinity (S), and carbon system variables:

$$\Omega = f(T, S, \text{DIC}, \text{ALK}), \quad (2)$$

where the function f refers to the CO2SYS thermodynamic equations. Anomalies $\Delta\Omega$ were computed for each sample relative to a reference value, Ω_0 :

$$\Delta\Omega = \Omega - \Omega_0. \quad (3)$$

We used the high-salinity coastal end-member (the CBB1 site) as our reference value and determined station specific deviations from the open waters of Buzzards Bay. The mean ($n = 18$) water properties for the CBB1 sampling station were used for the reference salinity, temperature, DIC, and ALK and were defined as $S_0 = \overline{S_{\text{CBB1}}}$, $T_0 = \overline{T_{\text{CBB1}}}$, $\text{DIC}_0 = \overline{\text{DIC}_{\text{CBB1}}}$, $\text{ALK}_0 = \overline{\text{ALK}_{\text{CBB1}}}$, respectively. The reference saturation state is then computed from:

$$\Omega_0 = f(T_0, S_0, DIC_0, ALK_0). \quad (4)$$

Note that the reference value Ω_0 (1.92) differs from the mean Ω for the CBB1 (1.91) site because of the use of the reference values and nonlinearities in the thermodynamic equations. The saturation state anomalies for all samples are then estimated by a linear Taylor series decomposition (e.g., Doney et al. 2009, Cai et al., 2017):

$$\Delta\Omega_X = \sum(\partial\Omega/\partial X)\Delta X, \quad (5)$$

summing the perturbation effects for multiple factors, where $\partial\Omega/\partial X$ is the partial derivative of saturation state with respect to generic variable X around the reference state, and ΔX is the deviation in X from the reference value X_0 following equation (3). Here, we consider the thermodynamic effects of temperature ($\Delta\Omega_T$) and salinity ($\Delta\Omega_S$), conservative mixing of DIC and ALK of the freshwater end-member ($\Delta\Omega_{\text{mix}}$), and biogeochemistry factors ($\Delta\Omega_{\text{BGC}}$), with the addition of an error term, ϵ , to account for unidentified processes and nonlinearities in the carbonate system:

$$\Delta\Omega = \Delta\Omega_T + \Delta\Omega_S + \Delta\Omega_{\text{mix}} + \Delta\Omega_{\text{BGC}} + \epsilon. \quad (6)$$

The individual terms are approximated numerically using the CO2SYS thermodynamic code, rather than explicitly determining $\partial\Omega/\partial X$. The first two terms for the temperature and salinity perturbations arise straightforwardly from the Taylor decomposition in equation (5):

$$\Delta\Omega_T = f(T, S_0, DIC_0, Alk_0) - \Omega_0, \quad (7)$$

$$\Delta\Omega_S = f(T_0, S, DIC_0, Alk_0) - \Omega_0. \quad (8)$$

The temperature and salinity terms reflect changes in Ω arising from variations in observed temperature, T , and observed salinity, S , on the thermodynamic coefficients in CO2SYS involved in K_{sp} and calculation of $[\text{CO}_3^{2-}]$ from DIC and ALK. The salinity term also accounts for the linear variation of $[\text{Ca}^{2+}]$ with salinity (equation (1)).

To account for correlation between ALK and DIC and strong dilution with freshwater (e.g., Fassbender et al., 2017) at inner harbor sampling stations, we use freshwater mixing ($\Delta\Omega_{\text{mix}}$) and biogeochemical ($\Delta\Omega_{\text{BGC}}$) terms rather than $\Delta\Omega_{\text{DIC}}$ and $\Delta\Omega_{\text{ALK}}$, as has been done in a number of other studies (e.g., Doney, Lima et al., 2009 for pCO_2 ; Wang et al., 2017; Xu et al., 2017 for Ω) or a combined biophysical term (e.g., Fassbender et al., 2018 for pCO_2). The mixing term reflects the effects on Ω of changes of DIC and ALK as a function of salinity for two-endmember conservative mixing determined for Buzzards Bay:

$$\Delta\Omega_{\text{mix}} = f(T_0, S_0, DIC_S, ALK_S) - \Omega_0, \quad (9)$$

where DIC_S and ALK_S are the estimated values at the observed sample salinity S based on freshwater and CBB1 endmembers. Mixing will be linear for DIC and ALK because they are conservative tracers, but the salinity-dilution curves for derived quantities such as Ω and pH will be nonlinear. The freshwater endmember was derived from measurements collected in the upper Agawam River, which flows into the Wareham River Estuary (Figure 1) and is one of the seven main river basins flowing into Buzzards Bay. Ideally, this analysis would include measurements of DIC and ALK from multiple freshwater sources to generate mixing curves for each embayment, but the additional freshwater sampling was beyond the scope of our study. We used the mean of samples from CBB1 as the coastal seawater endmember and for measurements where salinity was beyond the mean of CBB1, we extrapolate the DIC-S and ALK-S mixing lines, but note that the extrapolation distance is relatively small. To explore the influence of the choice of endmembers on our results, we used bootstrapping techniques to resample our fresh and seawater endmembers (see Text S1 and Figures S1–S3 in the supporting information).

The biogeochemical term can be estimated as the difference between the calculated Ω at the observed sample DIC, ALK, and salinity and the Ω from the dilution curve at the sample salinity:

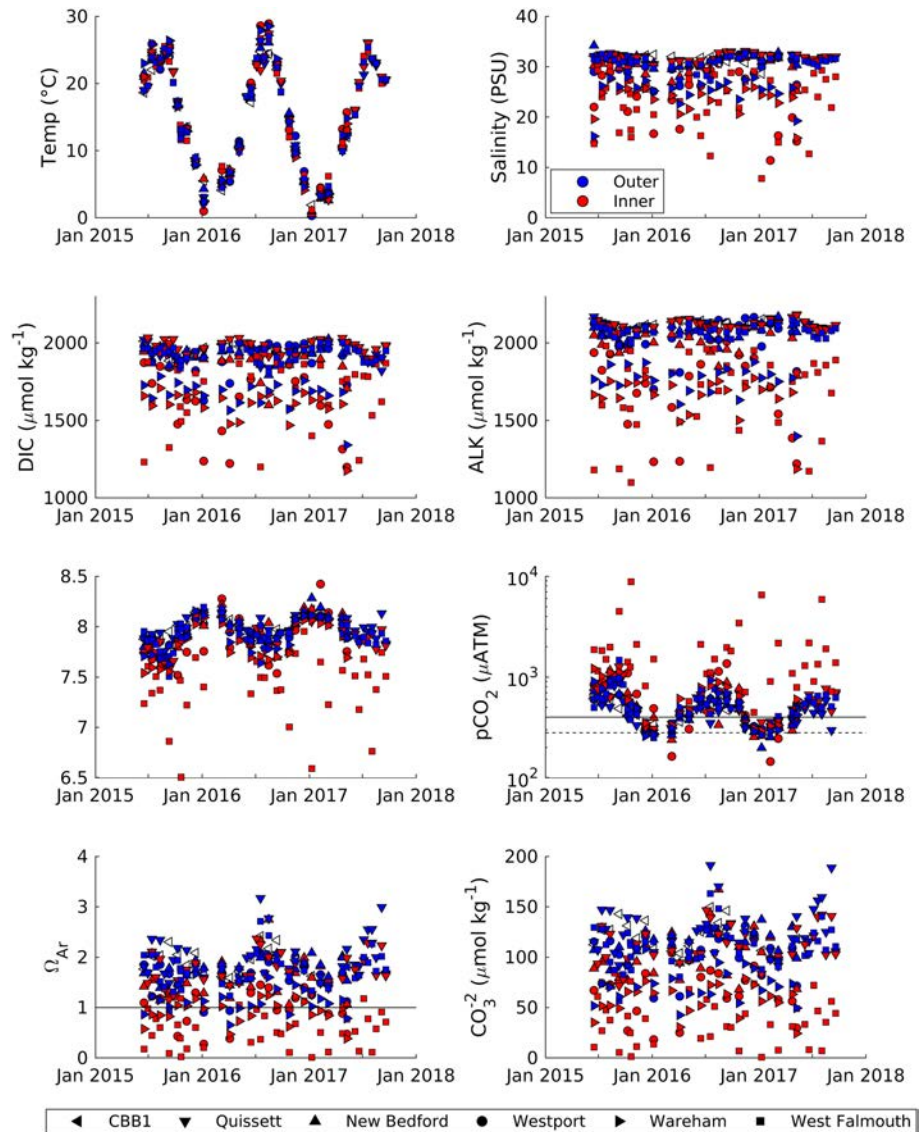


Figure 2. Time series of the carbonate chemistry dataset. Blue and red symbols designate outer and inner stations, respectively and individual embayments are given unique symbols. Dissolved inorganic carbon (DIC) and total alkalinity (ALK) were measured, and the full carbonate system parameters were calculated using CO2SYS v.1.3 (Lewis & Wallace 1998; van Heuven et al., 2011). The line on the aragonite saturate state panel indicates the critical thermodynamic equilibrium of 1. The line on the $p\text{CO}_2$ panel represents approximate atmospheric equilibrium of $400 \mu\text{ATM}$.

$$\Delta\Omega_{\text{BGC}} = f(T_0, S, \text{DIC}, \text{ALK}) - f(T_0, S, \text{DIC}_S, \text{ALK}_S), \quad (10)$$

where DIC, ALK, and S are the observed values. The direct estimate of four terms of equation (6) allows an explicit calculation of a residual term that arises from dropping the higher order terms in the linear Taylor decomposition (equation (5)) of a nonlinear thermodynamic system:

$$\varepsilon = \Delta\Omega - (\Delta\Omega_T + \Delta\Omega_S + \Delta\Omega_{\text{mix}} + \Delta\Omega_{\text{BGC}}). \quad (11)$$

3. Results and Discussion

3.1. Overall Patterns in Carbonate Chemistry

In most embayments, we observed measurable differences in both carbonate and nutrient chemistry between inner and outer harbor stations, where the generally fresher inner harbor stations tended to have lower DIC, ALK, pH, and Ω and higher $p\text{CO}_2$ (Figures 2, S6–S9, and S12) and nutrient concentrations (Figures 3, S14–

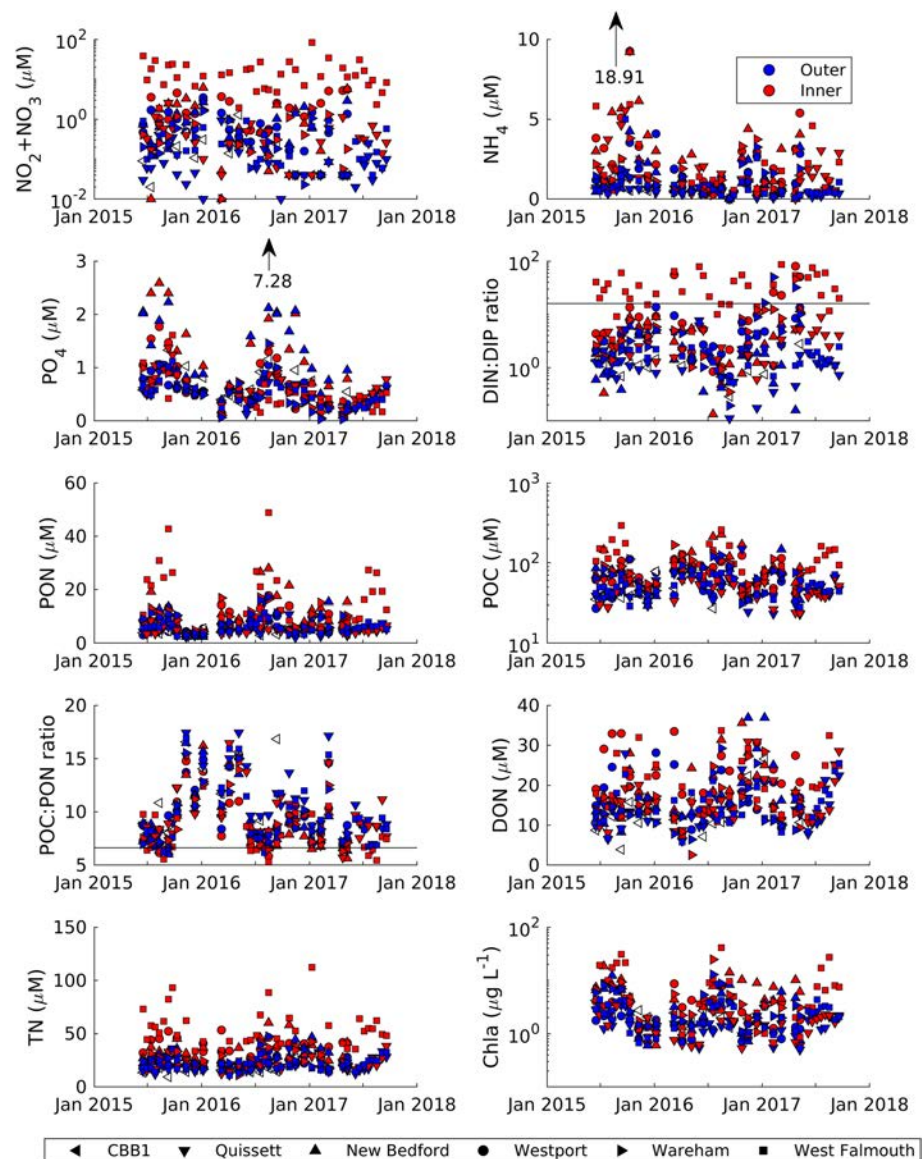


Figure 3. Time series of the nutrient chemistry dataset. Blue and red data points designate outer and inner stations, respectively and individual embayments are given unique symbols. Horizontal lines indicate Redfield DIN:DIP (16:1) and POC:PON (106:16) ratios.

S17, and S19) than outer harbor stations. Carbonate system measurements showed seasonal variations due to changes in DIC, ALK, and freshwater inputs as well as temperature dependence of calculated carbonate system parameters (e.g., pH, Ω ; Figure S2). Seasonal variability in DIC and ALK was evident at most sampling stations and was broadly consistent from year to year, although more years of monitoring would be necessary to define an accurate climatological seasonal cycle. Buzzards Bay source water exhibited higher DIC and ALK during winter than summer, and outer harbor stations generally followed a similar pattern (Figures 2, S6, and S7). Inner harbors exhibited less consistent seasonality in DIC and ALK but nearly always had lower pH, Ω , and higher pCO_2 than outer harbor stations during summer when biological activity was high (Figures 2, S8, S9, and S12).

We observed a strong correlation between DIC and ALK across all sampling stations and seasons. The first-order variability in these parameters was clearly related to freshwater inputs, as indicated by correlations of DIC and ALK with salinity (Figures 4 and 5). Freshwater samples from the upper Agawam River and the relatively high-salinity samples from the CBB1 station provided the endmembers for conservative mixing

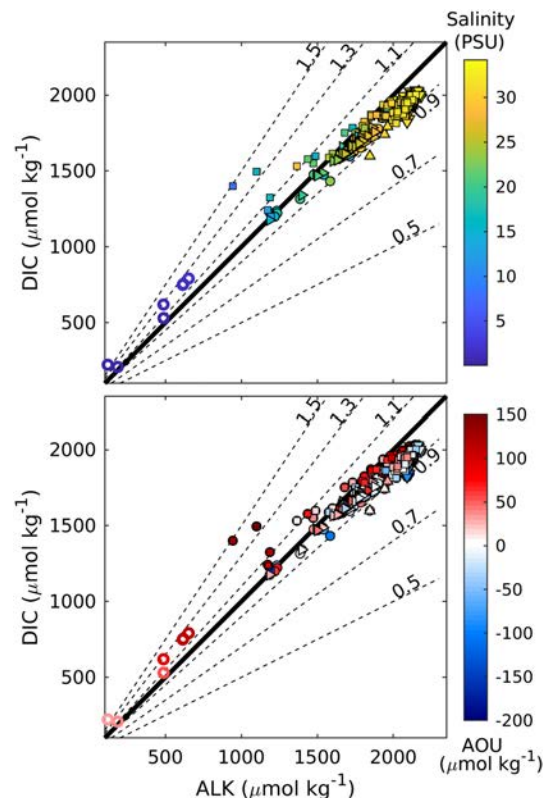


Figure 4. Dissolved inorganic carbon (DIC) vs. total alkalinity (ALK) for all samples. Data are colored by salinity (top panel) and apparent oxygen utilization (AOU, bottom panel). Symbols are unique for each embayment and correspond to the symbols in Figure 1. Open symbols were collected in the Agawam river. Thick line is 1:1, other ratios are indicated on the Figure.

lines for both DIC (slope: $45.8 \pm 0.07 \mu\text{mol kg}^{-1}/\text{PSU}$, intercept: $517 \pm 131 \mu\text{mol kg}^{-1}$) and ALK (slope: $54.6 \pm 0.05 \mu\text{mol kg}^{-1}/\text{PSU}$, intercept: $409 \pm 103 \mu\text{mol kg}^{-1}$; Figure 5). The DIC and ALK data (Figures 4 and 5) highlight a shift from basic conditions ($\text{ALK} > \text{DIC}$) for the Buzzards Bay coastal water endmember toward more acidic conditions ($\text{ALK} \leq \text{DIC}$) for the lower salinity inner harbor and Agawam River freshwater endmember, consistent with low-alkalinity freshwater sources typical of the U.S. Northeast (e.g., Liu et al., 2017).

The observed ratio of DIC to ALK was correlated to AOU ($r = -0.43$, $p < 0.0001$), reflecting CO_2 uptake or release and respiratory history (Figure 4). For samples with large positive AOU (i.e., O_2 uptake and CO_2 release due to both water column and benthic respiration), the DIC to ALK ratio approached 1 or was greater than 1, and thus sample Ω , $[\text{CO}_3^{2-}]$, and pH tended to fall well below their expected values based on the mixing curve and seasonal variations in temperature (Figures 4b and 6). Samples with large negative AOU (i.e., O_2 production and CO_2 drawdown due to primary production), tended to fall above the expected mixing curves while samples with AOU close to zero tended to fall near the mixing curve (Figure 6).

Our observations show that freshwater input is a strong driver of local carbonate chemistry, but that eutrophication also has a large influence; similar to results that have been reported by previous studies (e.g., Wallace et al., 2014, Ekstrom et al., 2015, Pimenta & Gear, 2018). At many of our inner harbor stations, we observed Ω values that seasonally approached 1.0 on a regular basis, and in West Falmouth Harbor, Ω was consistently at or below 1.0 all year (Figure 2). The overall pattern was similar for calcite saturation state but shifted to higher values by approximately 1 unit (not shown). Even with the lower solubility of calcite, stations with lower salinity also experienced calcite saturation state near or less than 1 occasionally (not shown). In addition to very low Ω , we also observed lower dissolved oxygen at inner harbor stations with concentrations as low as $105.5 \mu\text{mol kg}^{-1}$ and 49.6 % saturation, suggesting these environments experience both acidification and dissolved oxygen stresses.

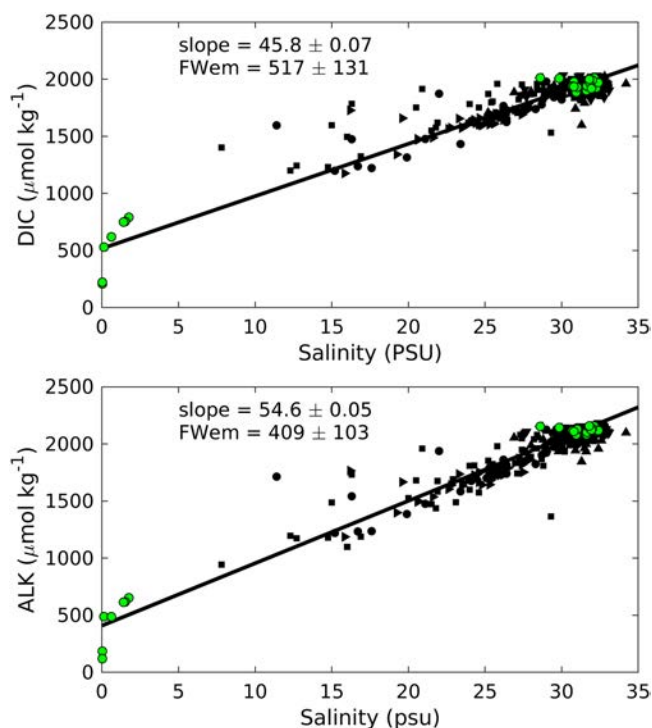


Figure 5. Dissolved inorganic carbon (DIC, top panel) and total alkalinity (ALK, bottom panel) plotted against salinity. Green points are samples from the two endmembers: low salinity samples are from the nontidal portion of the upper Agawam River, which feeds into the Wareham River Estuary, and high salinity samples are from CBB1 and individual embayments are given unique symbols. The line illustrates the anticipated mixing curve between the upper Agawam river and the open waters of Buzzards Bay.

Our sample collection was designed to target periods of high stress by sampling during the ebb tide and in the morning, potentially capturing higher freshwater discharge and less time for local production to take up DIC produced throughout the night. Higher temporal frequency measurements of pH at nearby locations suggest that local production during the day can increase pH by more than 1 unit and thus may raise Ω considerably compared to the morning, low tide conditions in this data set (see Howarth et al., 2014 for a time series from West Falmouth Harbor). Diurnal variations in pH driven by CO_2 production or consumption are usually coupled with concurrent variations in O_2 concentration that can lead not only to periods of multiple stresses (i.e., low pH, low Ω , and low O_2 at night) but also periods of beneficial conditions (i.e., high pH, high Ω , and high O_2 during the day) that may provide temporary refugia for sensitive species (Hendriks et al., 2014). However, recent experimental work on bay scallops and hard clams suggests diurnal variability in pH and O_2 simulating local production and respiration cycles does not in fact provide a refuge from acidification, and in some cases, organisms fared worse under fluctuating than chronic acidification conditions (Gobler et al., 2017).

3.2. Decomposition of Aragonite Saturation State

Developing an accurate understanding of the underlying drivers of coastal acidification is critical to determining effective management solutions. We chose to decompose Ω into four components to determine the relative contribution of temperature, salinity, freshwater mixing, and biogeochemistry on observed Ω . Figure 6b shows how these factors would affect the Ω of the Buzzards Bay study area where the reference station (CBB1) is shown by the black circle. Temperature-induced variation ($\Delta\Omega_T$) would shift Ω vertically, with lower Ω at lower T. A decrease in salinity ($\Delta\Omega_S$) from the S_0 value of CBB1 would lead to higher Ω , reflecting the offsetting effects of decreasing calcium ion concentration and K_{sp} and increases in $[\text{CO}_3^{2-}]$ at lower salinity due to changes in the dissociation coefficients K_1 and K_2 and in the activity coefficients of ions in solution. Freshwater mixing ($\Delta\Omega_{\text{mix}}$) would reduce Ω along the mixing curve because the freshwater endmember observed in Buzzards Bay was relatively acidic, with a DIC:ALK ratio greater than 1.

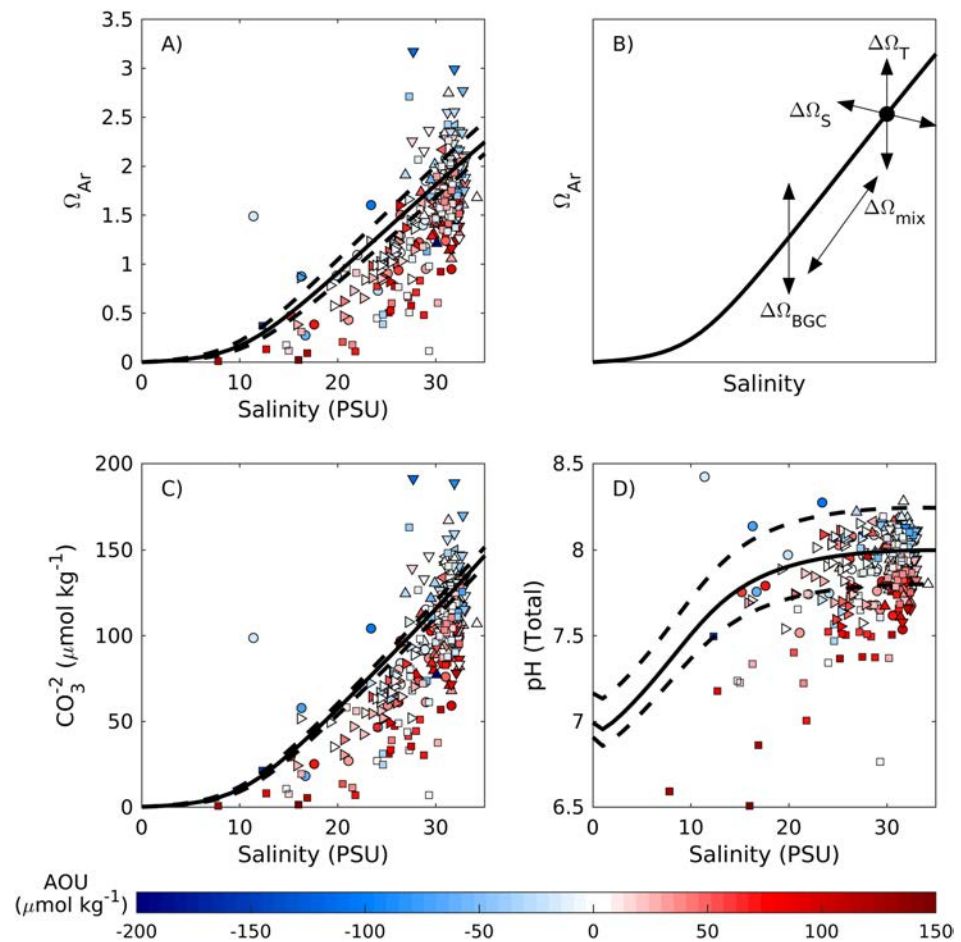


Figure 6. Top panels: aragonite saturation state (Ω) vs. salinity, and conceptual diagram illustrating the decomposition of Ω as a function of salinity. The solid line for all panels is calculated from the conservative mixing line for DIC and ALK using the dataset mean temperature, while dashed lines are calculated using the maximum and minimum observed temperatures. The dot indicates the CBB1 reference station. Each perturbation process is shown as $\Delta\Omega_x$, where $\Delta\Omega_x$ describes the perturbation of Ω due to temperature (T), salinity (S), conservative freshwater mixing (mix), and biogeochemical processes (BGC) (equations (6)–(10)). Arrows indicate the expected direction caused by each perturbation process. Bottom panels: carbonate ion concentration (CO_3^{2-}), and pH vs. salinity with the lines calculated as above from the conservative mixing lines. All points are colored by apparent oxygen utilization (AOU). Data points are given unique symbols that represent specific embayments that are consistent in the figures throughout the manuscript.

Note that Ω vs. salinity mixing curves will be different in environments with high-alkalinity freshwater endmembers, such as those receiving waters from glacial runoff (e.g., Tank et al., 2016) or regions with different bedrock geology (e.g. Cai & Wang, 1998). Local biogeochemistry ($\Delta\Omega_{\text{BGC}}$) would shift Ω vertically with no change in salinity, with the sign and magnitude of this change dependent on the stoichiometry of the metabolic processes (e.g., Soetaert et al., 2007). Each sample's overall perturbation from the coastal source water ($\Delta\Omega_{\text{Total}}$) is assumed to be a combination of these four factors and a residual term (ϵ) that includes any unaccounted for processes and limitations of linear approximations of nonlinear systems.

The term $\Delta\Omega_{\text{Total}}$ varied both between embayments and within each embayment, and inner harbor stations typically had larger negative $\Delta\Omega_{\text{Total}}$ than outer harbor stations (Figure 7). Temperature and salinity had a relatively small overall impact on the observed range of $\Delta\Omega_{\text{Total}}$, a result consistent with similar analyses of Mid-Atlantic Bight shelf/slope waters (Xu et al., 2017). However, at outer harbor stations where Buzzards Bay water had a large influence on the local carbonate system but the overall variation in Ω was small, seasonal variability in temperature and salinity caused $\Delta\Omega_{\text{T}}$ and $\Delta\Omega_{\text{S}}$ to, in a few cases, be of a similar magnitude as $\Delta\Omega_{\text{Total}}$ (e.g., outer Quissett). Freshwater mixing had a clear and very strong control on the

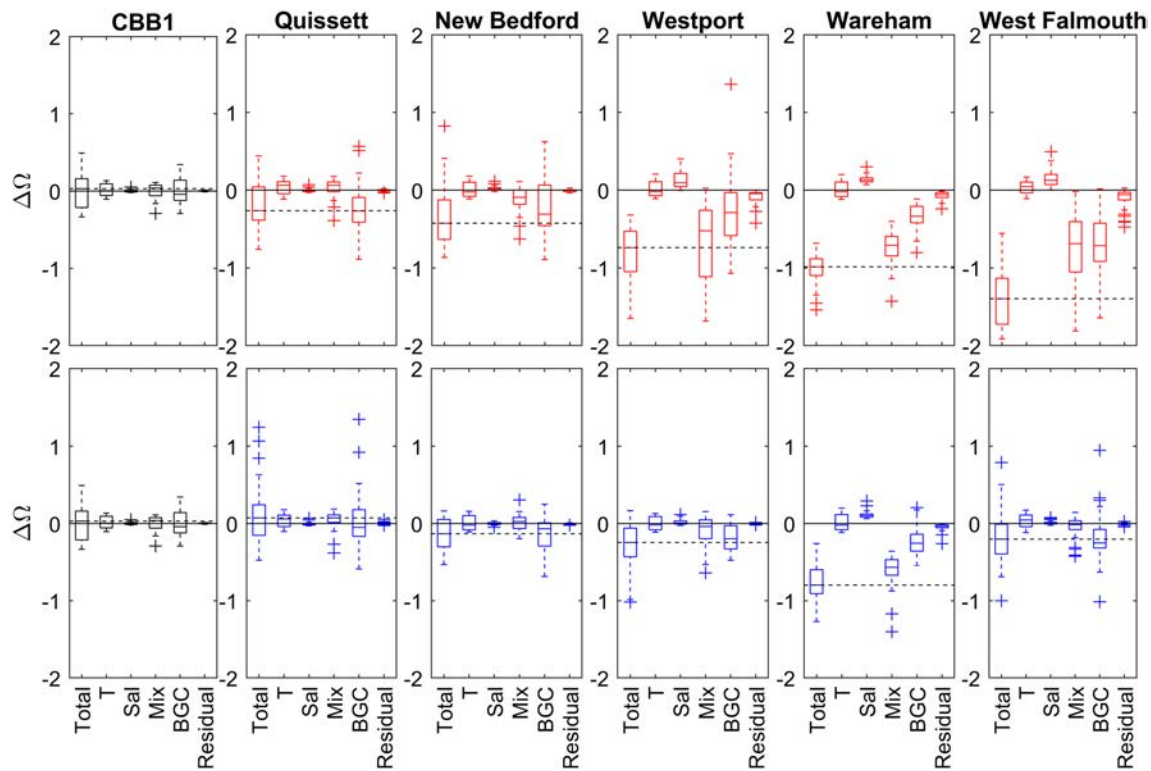


Figure 7. Distributions of the components of the aragonite saturation state ($\Delta\Omega_x$) decomposition (equation (6)) as: the total perturbation from the CBB1 reference station (Total), the perturbations due to temperature (T), salinity (S), freshwater mixing (Mix), and biogeochemical processes (BGC), and the estimated residual term (Residual). Bottom panels (blue) are from outer harbors, and top panels (red) are from inner harbor stations, the far left panels in both the top and bottom rows are from the CBB1 reference station. Dashed lines indicate the median $\Delta\Omega_{\text{Total}}$ for each sampling station.

variations in Ω where $\Delta\Omega_{\text{mix}}$ was consistent with differences in salinity and expected freshwater discharge across embayments. Stations with high surface or groundwater discharge tended to have relatively low salinity (Westport, Wareham, and West Falmouth inner harbor stations), and thus larger $\Delta\Omega_{\text{mix}}$ (Figure 7). The residual term was correlated to salinity such that the magnitude was larger for fresher measurements, but for the majority of our samples, the residual term was small relative to the magnitude of $\Delta\Omega_{\text{Total}}$ (Figures 7 and S5).

In most embayments, $\Delta\Omega_{\text{BGC}}$ was a large component of $\Delta\Omega_{\text{Total}}$. Outer harbor stations tended to have smaller $\Delta\Omega_{\text{BGC}}$ than inner harbor stations, due to carbonate system chemistry that was similar to the open waters of Buzzards Bay, yielding smaller deviations from the estimated mixing curves. $\Delta\Omega_{\text{BGC}}$ is likely driven by a combination of the relative magnitudes of metabolic fluxes and the local water residence times. Small metabolic fluxes with short residence times would yield small $\Delta\Omega_{\text{BGC}}$, while increasing metabolic fluxes in the same location would increase $\Delta\Omega_{\text{BGC}}$. Small flux rates in locations with long residence times may also lead to increased $\Delta\Omega_{\text{BGC}}$, and we would expect large flux rates in areas of long residence time to lead to the largest $\Delta\Omega_{\text{BGC}}$. We observed correlations between station AOU and $\Delta\Omega_{\text{BGC}}$ ($r = -0.46$, $p < 0.0001$, all data; $r = -0.57$, $p < 0.0001$, summer, Figure 8), consistent with biological processes being the driver of the $\Delta\Omega_{\text{BGC}}$ component, especially during periods of warmer water temperatures and likely higher biological activity. The slope of the observations during warm periods (temperature $> 15^\circ\text{C}$, $-0.0056 \pm 0.0007 \Delta\Omega_{\text{BGC}}/\text{AOU}$, $(1/(\mu\text{mol kg}^{-1}))$) was also consistent with aerobic respiration and production using a Redfield ratio of DIC and ALK to O_2 ($-0.0097 \Delta\Omega_{\text{BGC}}/\text{AOU}$, $(1/(\mu\text{mol kg}^{-1}))$; Figure 8).

Although summertime $\Delta\Omega_{\text{BGC}}$ was consistent with oxygen production and aerobic respiration there was still considerable variation, especially in samples collected during cooler temperatures, that could be driven by other processes. First, our dilution curves do not capture embayment-specific or seasonal variability in end-member composition. In particular, it is possible that the carbonate chemistry of freshwater endmembers for

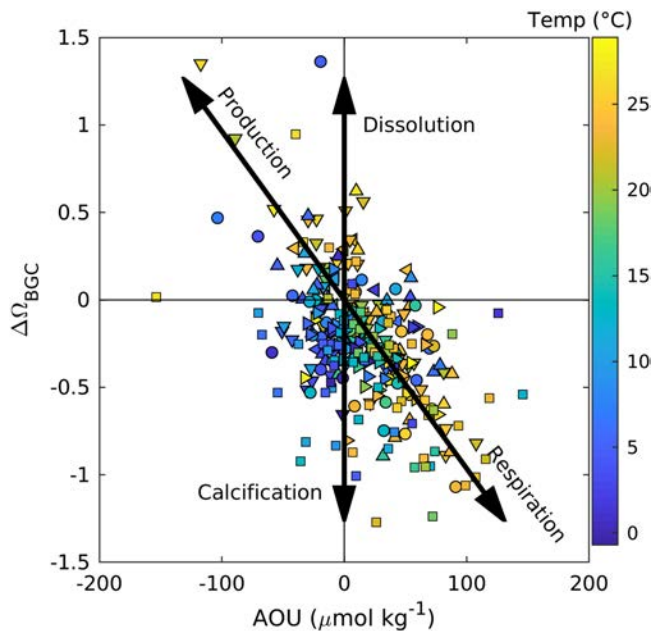


Figure 8. The perturbation due to biogeochemical processes ($\Delta\Omega_{BGC}$) plotted against apparent oxygen utilization (AOU). Data points are colored by temperature. The line for production and respiration reflects the expected slope based on a Redfield ratio of DIC and ALK to O_2 (1: -1, and -16: -106, respectively). Calcification or dissolution will respond to Ω , but the processes are not linked to AOU.

embayments across Buzzards Bay differs substantially from the Agawam River source water used here or that there may also be seasonal changes in surface or groundwater endmember DIC or ALK values. Both of these situations could lead to changes in the relative magnitudes of $\Delta\Omega_{mix}$ or $\Delta\Omega_{BGC}$ by altering the freshwater endmember of the dilution curve. The freshwater endmember DIC and ALK values from the upper Agawam River (517 ± 131 and 409 ± 103 for DIC and ALK, respectively, $n = 6$) agreed well with riverine carbonate chemistry data from the GLORICH database (Hartmann et al., 2019, see Text S3) averaged from a 100 km radius surrounding Buzzards Bay (665 ± 279 and 473 ± 225 [SD, $n = 16$ stations] for DIC and ALK, respectively). A bootstrapping error analysis found that the $\Delta\Omega_{BGC}$ term was not sensitive to varying the mean freshwater and seawater endmember DIC and ALK within the observed range (e.g., $\pm 0.045 \Omega$ units, see Text S1, Figures S1–S3). Additionally, for simplicity in this analysis, we used a single seawater endmember calculated from the mean DIC, ALK, S, and T measured in the open waters of Buzzards Bay. We did observe seasonality in the Buzzards Bay (CBB1) data and outer harbor measurements (Figures 2, S6–S9, and S12), which could indicate seasonal variation in either the coastal water masses or biogeochemical fluxes that inherently alter the carbonate chemistry of the Buzzards Bay source seawater. However, these observed seasonal variations are relatively small, and reanalyzing the dataset with a seasonally varying seawater endmember did not substantially change the results of this analysis (data not shown). Furthermore, we do not believe we have enough data from individual embayments to generate seasonal or embayment-specific dilution curves.

Second, anaerobic biological processes such as denitrification or sulfate reduction, nonbiological redox reactions, or significant calcification or dissolution may alter the seawater DIC:ALK ratio (Cai et al., 2017; Glud, 2008; Liu et al., 2017; Soetaert et al., 2007) and thus lead to the variability observed in the $\Delta\Omega_{BGC}$ to AOU relationship. These processes could occur in the water column or sediments, which often represent a large portion of the total ecosystem fluxes in shallow coastal environments (e.g., Long et al., 2019). The bulk water column measurements collected for this study integrate the effects of both water column and sedimentary

processes but do not allow us to estimate the relative contribution of sediments and water column processes to the $\Delta\Omega_{BGC}$ term. Although we highlight the correlation between $\Delta\Omega_{BGC}$ and AOU as an indication of one possible biological process affecting the $\Delta\Omega_{BGC}$ term, the analysis described below does not rely on the relationship between $\Delta\Omega_{BGC}$ and AOU relationship in any way nor do we make any assumptions on the underlying process driving the observed patterns.

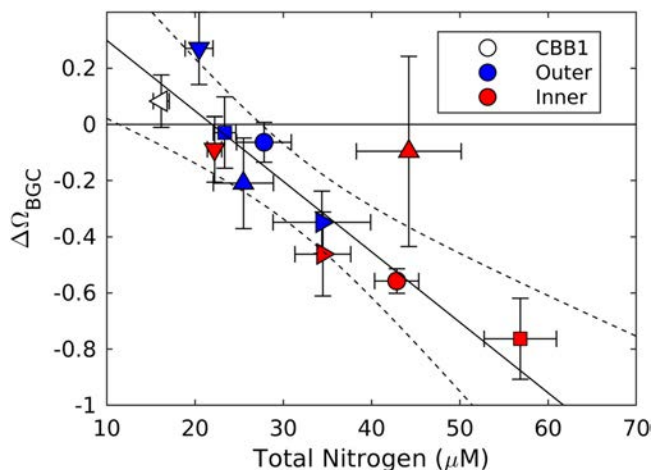


Figure 9. Station July/August average $\Delta\Omega_{BGC}$ vs. total nitrogen (TN) concentration. Blue points are outer harbors, red points are inner harbors, and the open point is the reference CBB1 station. Error bars are standard error. Symbols reflect individual embayments consistent with those given in the figures throughout the manuscript.

3.3. Influence of Eutrophication on Aragonite Saturation State

Regardless of the mechanism, we hypothesize that of the set of factors we use to describe Ω , the $\Delta\Omega_{BGC}$ term is most likely influenced by eutrophication. We observed a strong correlation between July and August station mean $\Delta\Omega_{BGC}$ and mean TN concentration ($r = -0.82$, $p = 0.002$, Figure 9). Since TN concentration reflects eutrophication status in coastal Buzzards Bay (Rheuban et al., 2016), this is consistent with a strong eutrophication influence on $\Delta\Omega_{BGC}$. Annual mean $\Delta\Omega_{BGC}$ was also strongly correlated to annual mean TN ($r = -0.85$, $p = 0.001$, not shown), but we focus our analysis on summer mean $\Delta\Omega_{BGC}$ and TN because historical measurements of water quality in Buzzards Bay were typically only collected during the summer, and regional water quality

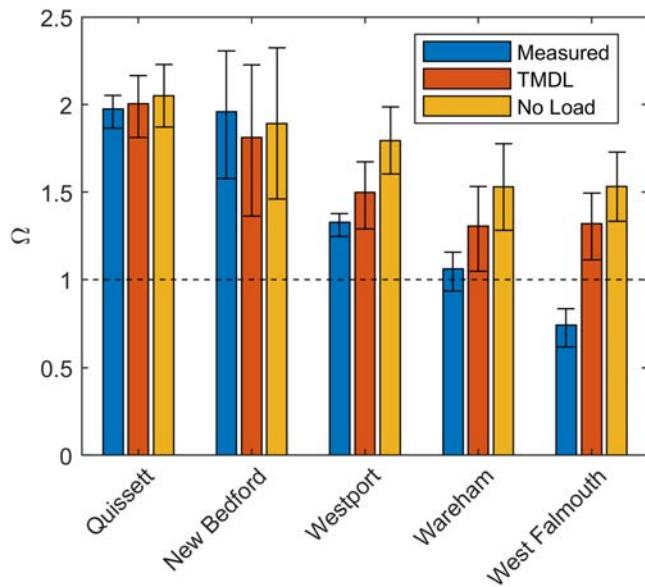


Figure 10. Average aragonite saturation state (Ω) from observations (blue) and estimated based on two nitrogen loading reduction scenarios: the total maximum daily load (TMDL, red) and no anthropogenic nitrogen loading (yellow). TN concentration was obtained from reports for each harbor generated through the Massachusetts Estuaries Project. TN was determined through water quality modeling based on nitrogen loads at proposed TMDLs and no anthropogenic nitrogen loading scenarios. Dashed line illustrates $\Omega = 1$. Error bars are standard error, estimated by propagating the variability in observed Ω , the uncertainty associated with the DIC and ALK mixing curves, and the uncertainty in the relationship between total nitrogen concentration (TN) and $\Delta\Omega_{BGC}$.

modeling efforts use summertime data for model validation and future scenario projections.

The pattern in both TN and $\Delta\Omega_{BGC}$ followed expected nitrogen loading gradients (Figure 9); bays with high nitrogen loading and resultant high rates of respiration and organic matter decomposition had strongly negative $\Delta\Omega_{BGC}$ values. Within-embayment variation (inner vs. outer harbor $\Delta\Omega_{BGC}$) was also consistent with this mechanism, with inner harbors tending to fall further from the Buzzards Bay reference station (Figure 9). The inner station in New Bedford was the exception to this relationship, in part because we observed very different chemistry in summer 2015 and in summer 2016. In 2016, DIC and ALK at the inner station were much lower than expected based on the observed salinity. The 2016 DIC:ALK ratio was also lower than in 2015, leading to Ω that was considerably higher (2.54 ± 0.29 , summer 2016) than observed during other sampling periods in New Bedford (1.35 ± 0.28 for summer 2015, 1.57 ± 0.42 across all data). The inner New Bedford mean from 2015 agreed well with other measurements but without an understanding of the cause of the summer 2016 persistent high Ω , we hesitate to exclude it from our analysis. This high degree of variability between the two summers sampled in New Bedford illustrates the importance of long-term monitoring of the coastal carbonate and nutrient systems in order to fully develop baseline climatologies that will allow for the exploration of potential future change.

Regional water quality managers have very little control over temperature, salinity, and freshwater mixing; however, state and local managers can use the regulatory framework of the Clean Water Act to reduce nitrogen pollution and the negative consequences of eutrophication. As part of statewide efforts to improve coastal water quality, the MEP (<https://www.mass.gov/guides/the-massachusetts-estuaries-project-and-reports>) was designed to evaluate estuarine health and develop TMDLs for approximately 70 embayments across the Massachusetts coastline, including the five embayments sampled as part of this study (Howes et al., 2006, 2012, 2013, 2014, 2015). These MEP reports modeled TN concentration under proposed future nitrogen loading scenarios at most of our sampling stations because the MEP process used the same Buzzards Bay Coalition historical data and sampling stations as validation for their water quality modeling efforts. Using modeled TN concentrations, the relationship observed between $\Delta\Omega_{BGC}$ and TN (Figure 9) can then provide an estimate of the impacts of future nitrogen loading reduction scenarios on station Ω . Of the five harbors sampled, four of the inner stations show projected increases in Ω under both the reduced nitrogen loading TMDL and the “no anthropogenic

mass.gov/guides/the-massachusetts-estuaries-project-and-reports) was designed to evaluate estuarine health and develop TMDLs for approximately 70 embayments across the Massachusetts coastline, including the five embayments sampled as part of this study (Howes et al., 2006, 2012, 2013, 2014, 2015). These MEP reports modeled TN concentration under proposed future nitrogen loading scenarios at most of our sampling stations because the MEP process used the same Buzzards Bay Coalition historical data and sampling stations as validation for their water quality modeling efforts. Using modeled TN concentrations, the relationship observed between $\Delta\Omega_{BGC}$ and TN (Figure 9) can then provide an estimate of the impacts of future nitrogen loading reduction scenarios on station Ω . Of the five harbors sampled, four of the inner stations show projected increases in Ω under both the reduced nitrogen loading TMDL and the “no anthropogenic

Table 2
Calculated $\Delta\Omega_{BGC}$, Total Nitrogen (TN) Concentration and Aragonite Saturation State (Ω) at Inner Harbor Stations

| | | Quissett | New bedford | Westport | Wareham | West falmouth |
|----------|----------------------|------------------|------------------|------------------|------------------|------------------|
| Observed | $\Delta\Omega_{BGC}$ | -0.09 ± 0.12 | -0.10 ± 0.34 | -0.56 ± 0.04 | -0.46 ± 0.15 | -0.76 ± 0.14 |
| | TN (μM) | 22.2 ± 0.8 | 44.2 ± 5.9 | 42.9 ± 2.5 | 34.5 ± 3.2 | 56.9 ± 4.1 |
| | Ω | 1.96 ± 0.09 | 1.94 ± 0.36 | 1.31 ± 0.07 | 1.05 ± 0.11 | 0.73 ± 0.10 |
| TMDL | $\Delta\Omega_{BGC}$ | -0.06 ± 0.07 | -0.24 ± 0.06 | -0.39 ± 0.06 | -0.22 ± 0.06 | -0.19 ± 0.06 |
| | TN (μM) | 24.27 | 31.62 | 34.4 | 30.62 | 29.41 |
| | Ω | 2.01 ± 0.18 | 1.81 ± 0.43 | 1.50 ± 0.19 | 1.31 ± 0.24 | 1.32 ± 0.19 |
| No Load | $\Delta\Omega_{BGC}$ | -0.01 ± 0.07 | -0.16 ± 0.06 | -0.09 ± 0.07 | 0.01 ± 0.08 | 0.02 ± 0.08 |
| | TN (μM) | 22.48 | 28.41 | 25.55 | 21.7 | 20.99 |
| | Ω | 2.05 ± 0.18 | 1.89 ± 0.43 | 1.79 ± 0.19 | 1.53 ± 0.25 | 1.53 ± 0.20 |

Note. Observed values are July/August means from this study. TN concentrations for the total maximum daily load (TMDL) and No Load scenarios for each of the harbors are from Howes et al. (2006, 2012, 2013, 2014, 2015). Error shown is standard error ($n = 12, 4, 4, 12$, respectively). $\Delta\Omega_{BGC}$ for the TMDL and No Load scenarios is determined from the TN concentration and the relationship in Figure 10. Ω is then estimated from equations (6) and (3).

load” scenarios, with the exception of New Bedford inner harbor, which shows declines that are not statistically different than the observations (Figure 10, Table 2). Harbors with better water quality, higher observed Ω , and lower present-day estuary-volume-normalized nutrient loads see smaller or little improvement. We estimate that Ω in morning, low-tide conditions in the most eutrophic estuaries may increase (i.e., improve) by nearly 0.5 units under a TMDL scenario, and more than 0.6 units under a no anthropogenic load scenario (Figure 10, Table 2).

These projected increases in station summer mean Ω could lead to dramatic improvements in West Falmouth and Wareham inner harbors in particular, where Ω may increase from conditions close to or well below an Ω of 1 to above the critical thermodynamic equilibrium (Figure 10). Our sampling program was designed to target the periods with the greatest stresses (morning, low-tide), and as it is possible that our seawater endmember is also influenced by eutrophication, these improvements would represent a conservative lower bound for average Ω in these bays. Model estimates for the northeast shelf suggest that Ω has declined by more than 0.5 units since the industrial revolution (Feely et al., 2009, Environmental Protection Agency (EPA), 2016). A simple calculation of changes to Ω for Buzzards Bay from preindustrial conditions (see Text S2) illustrates that the Ω improvements (e.g., increases) that could be achieved through reduced nitrogen loading at the most eutrophic stations are likely to be larger than the Ω declines associated with past or near-future atmospheric CO_2 increases (Table S1). Many shellfish species important to the culture and economy of the U.S. Northeast, e.g., hard clam, eastern oyster, and bay scallop, have shown sensitivity to Ω (see summary in Gledhill et al., 2015) and most laboratory studies show that lowered Ω values lead to reduced growth, calcification, or survival rates even for experimental conditions with Ω larger than 1. Thus, these potential improvements to Ω could facilitate improved shellfish survival and growth even for embayments not yet undersaturated with respect to aragonite.

4. Conclusions

Application of management strategies to improve coastal acidification is complex, as there are many drivers that determine local carbonate chemistry. Furthermore, developing regulatory loading limits through the Clean Water Act for dissolved carbon in coastal environments is not likely a suitable strategy to improve coastal acidification. However, the connection between eutrophication and coastal acidification is clear (Cai et al., 2011; Howarth et al., 2011; Wallace et al., 2014; Pimenta & Grear 2018). As a result, more immediate and larger improvements to the coastal acidification problem can likely be gained by reducing eutrophication and the subsequent organic matter respiration and CO_2 release. Additionally, in highly eutrophic estuaries, the increases to Ω gained through nutrient management could be larger than the estimated decline associated with a change from preindustrial atmospheric CO_2 to present day conditions and up to nine fold larger than those associated with Ω declines expected over the next decade due to atmospheric CO_2 trends (Table S1). The quantitative framework described in this study allowed us to estimate the relationship between proxies for nitrogen loading and coastal acidification in order to predict the possible improvements in coastal carbonate chemistry following nitrogen loading reduction scenarios. We envision this framework will be useful for local and regional decision making to allow quantitative metrics of potential improvements in coastal acidification to be incorporated in the discussion of nutrient impairment and TMDL attainment strategies.

References

- Alin, S. R., Feely, R. A., Dickson, A. G., Hernandez-Ayon, J. M., Juranek, L. W., Ohman, M. D., & Goericke, R. (2012). Robust empirical relationships for estimating the carbonate system in the southern California Current System and application to CalCOFI hydrographic cruise data (2005-2011). *Journal of Geophysical Research*, *117*, C05033. <https://doi.org/10.1029/2011JC007511>
- Barton, A., Hales, B., Waldbusser, G. G., Langdon, C., & Feely, R. A. (2012). The Pacific oyster, *Crassostrea gigas*, shows negative correlation to naturally elevated carbon dioxide levels: Implications for near-term ocean acidification effects. *Limnology and Oceanography*, *57*(3), 698–710. <https://doi.org/10.4319/lo.2012.57.3.0698>
- Bopp, L., Resplandy, L., Orr, J. C., Doney, S. C., Dunne, J. P., Gehlen, M., et al. (2013). Multiple stressors of ocean ecosystems in the 21st century: Projections with CMIP5 models. *Biogeosciences*, *10*, 6225–6245. <https://doi.org/10.5194/bg-10-6225-2013>
- Cai, W. J., Hu, X., Huang, W. J., Murrell, M. C., Lehrter, J. C., Lorenz, S. E., et al. (2011). Acidification of subsurface coastal waters enhanced by eutrophication. *Nature Geoscience*, *4*(11), 766–770. <https://doi.org/10.1038/ngeo1297>
- Cai, W. J., Huang, W. J., Luther, G. W. III, Pierrot, D., Li, M., Testa, J., et al. (2017). Redox reactions and weak buffering capacity lead to acidification in the Chesapeake Bay. *Nature Communications*, *8*, 369. <https://doi.org/10.1038/s41467-017-00417-7>
- Cai, W. J., & Wang, Y. (1998). The chemistry, fluxes, and sources of carbon dioxide in the estuarine waters of the Satilla and Altamaha Rivers, Georgia. *Limnology and Oceanography*, *43*(4), 657–668. <https://doi.org/10.4319/lo.1998.43.4.0657>

Acknowledgments

We thank Kelly Luis, Michaela Fendrock, Will Oesterich, Sheron Luk, Marti Jeglinksi, and Tony Williams for their help with field sample collection and logistical support and Chris Neill, Lindsay Scott, Rich McHorney, and Paul Henderson for laboratory sample analysis. We also thank the Waquoit Bay National Estuarine Research Reserve for loaning their handheld water quality meters and two anonymous reviewers for their feedback on this manuscript. Financial support for this work was provided by the John D. and Catherine T. MacArthur Foundation (grant no. 14-106159-000-CFP), MIT Sea Grant (subaward 5710004045) and the West Wind Foundation. The data used in this analysis can be found in the NOAA NCEI repository for carbonate chemistry measurements, the Ocean Carbon Data System at the following link: <https://www.nodc.noaa.gov/ocads/data/0206206.xml>.

- Cape Cod Commission (2015). *Cape Cod area wide water quality management plan update, June 2015*. MA: Barnstable. https://www.capecodcommission.org/resource-library/file/?url=/dept/commission/team/Website_Resources/208/2017_Implementation_Report_208_Addendum.pdf
- Cape Cod Commission (2017). *Addendum to the Cape Cod area wide water quality management plan update, August 2017*. Barnstable, MA. http://www.capecodcommission.org/resources/208/2017_Implementation_Report_208_Addendum.pdf
- Cooley, S. R., & Doney, S. C. (2009). Anticipating ocean acidification's economic consequences for commercial fisheries. *Environmental Research Letters*, 4(2), 024007. <https://doi.org/10.1088/1748-9326/4/2/024007>
- Cooley, S. R., Lucey, N., Kite-Powell, H., & Doney, S. C. (2012). Nutrition and income from molluscs today imply vulnerability to ocean acidification tomorrow. *Fish and Fisheries*, 13(2), 182–215. <https://doi.org/10.1111/j.1467-2979.2011.00424.x>
- Cooley, S. R., Rheuban, J. E., Hart, D. R., Luu, V., Glover, D. M., Hare, J. A., & Doney, S. C. (2015). An integrated assessment model for helping the United States sea scallop (*Placopecten magellanicus*) fishery plan ahead for ocean acidification and warming. *PLoS ONE*, 10(5), e0124145. <https://doi.org/10.1371/journal.pone.0124145>
- Dickson, A. G. (1990). Thermodynamics of the dissociation of boric acid in synthetic seawater from 273.15 to 318.15 K. *Deep Sea Research Part A: Oceanographic Research Papers*, 37(5), 755–766. [https://doi.org/10.1016/0198-0149\(90\)90004-F](https://doi.org/10.1016/0198-0149(90)90004-F)
- Doney, S. C., Balch, W. M., Fabry, V. J., & Feely, R. A. (2009). Ocean acidification: A critical emerging problem for the ocean sciences. *Oceanography*, 22(4), 16–25. <https://doi.org/10.5670/oceanog.2009.93>
- Doney, S. C., Lima, I., Feely, R. A., Glover, D. M., Lindsay, K., Mahowald, N., et al. (2009). Mechanisms governing interannual variability in upper-ocean inorganic carbon system and air-sea CO₂ fluxes: Physical climate and atmospheric dust. *Deep Sea Research Part II: Topical Studies in Oceanography*, 56(8–10), 640–655. <https://doi.org/10.1016/j.dsr2.2008.12.006>
- Ekstrom, J. A., Suatoni, L., Cooley, S. R., Pendleton, L. H., Waldbusser, G. G., Cinner, J. E., et al. (2015). Vulnerability and adaptation of US shellfisheries to ocean acidification. *Nature Climate Change*, 5(3), 207–214. <https://doi.org/10.1038/nclimate2508>
- Environmental Protection Agency (EPA) (2016). Climate change indicators in the United States: Ocean Acidity. <http://www.epa.gov/climate-indicators%20Updated%20August%202016>
- Fassbender, A. J., Alin, S. R., Feely, R. A., Sutton, A. J., Newton, J. A., & Byrne, R. H. (2017). Estimating total alkalinity in the Washington State coastal zone: Complexities and surprising utility for ocean acidification research. *Estuaries and Coasts*, 40(2), 404–418. <https://doi.org/10.1007/s12237-016-0168-z>
- Fassbender, A. J., Rodgers, K. B., Palevsky, H. I., & Sabine, C. L. (2018). Seasonal asymmetry in the evolution of surface ocean pCO₂ and pH thermodynamic drivers and the influence on sea-air CO₂ flux. *Global Biogeochemical Cycles*, 32(10), 1476–1497. <https://doi.org/10.1029/2017GB005855>
- Feely, R. A., Doney, S. C., & Cooley, S. R. (2009). Ocean Acidification: Present conditions and future changes in a high CO₂ world. *Oceanography*, 22(4), 36–47. <https://doi.org/10.5670/oceanog.2009.95>
- Gledhill, D. K., White, M. M., Salisbury, J., Thomas, H., Mlsna, I., Liebman, M., et al. (2015). Ocean and coastal acidification off New England and Nova Scotia. *Oceanography*, 28(2), 182–197. <https://doi.org/10.5670/oceanog.2015.41>
- Glud, R. N. (2008). Oxygen dynamics of marine sediments. *Marine Biology Research*, 4(4), 243–289. <https://doi.org/10.1080/17451000801888726>
- Gobler, C. J., Clark, H. R., Griffith, A. W., & Lusty, M. W. (2017). Diurnal fluctuations in acidification and hypoxia reduce growth and survival of larval and juvenile bay scallops (*Argopecten irradians*) and hard clams (*Mercenaria mercenaria*). *Frontiers in Marine Science*, 3, 282. <https://doi.org/10.3389/fmars.2016.00282>
- Hare, J. A., Morrison, W. E., Nelson, M. W., Stachura, M. M., Teeters, E. J., Griffis, R. B., et al. (2016). A vulnerability assessment of fish and invertebrates to climate change on the Northeast U.S. Continental Shelf. *PLoS ONE*, 11(2), e0146756. <https://doi.org/10.1371/journal.pone.0146756>
- Hartmann, J., Lauerwald, R., & Moosdorf, N. (2019). GLORICH—Global river chemistry database, PANGAEA <https://doi.org/10.1594/PANGAEA.902360>
- Hendriks, I. E., Olsen, Y. S., Ramajo, L., Basso, L., Steckbauer, A., Moore, T. S., et al. (2014). Photosynthetic activity buffers ocean acidification in seagrass meadows. *Biogeosciences*, 11(2), 333–346. <https://doi.org/10.5194/bg-11-333-2014>
- Howarth, R., Chan, F., Conley, D. J., Garnier, J., Doney, S. C., Marino, R., & Billen, G. (2011). Coupled biogeochemical cycles: eutrophication and hypoxia in temperate estuaries and coastal marine ecosystems. *Frontiers in Ecology and the Environment*, 9(1). <https://doi.org/10.1890/100008>
- Howarth, R. W., Hayn, M., Marino, R. M., Ganju, N., Foreman, K., McGlathery, K., et al. (2014). Metabolism of a nitrogen-enriched coastal marine lagoon during the summertime. *Biogeochemistry*, 118(1–3), 1–20. <https://doi.org/10.1007/s10533-013-9901-x>
- Howes, B., Eichner, E., Acker, R., Samimy, R., Ramsey, J., & Schlezinger, D. (2012). *Massachusetts estuaries project linked watershed-embayment approach to determine critical nitrogen loading thresholds for the westport river embayment system*. Boston, MA: town of Westport, MA, Massachusetts Department of Environmental Protection.
- Howes, B., Kelley, S. W., Ramsey, J. S., Eichner, E., Samimy, R., Schlezinger, D., & Detjens, P. (2013). *Massachusetts estuaries project linked watershed-embayment approach to determine critical nitrogen loading thresholds for the Quissett Harbor Embayment Systems, Town of Falmouth*. Boston, MA: Massachusetts Department of Environmental Protection.
- Howes, B., Kelley, S. W., Ramsey, J. S., Samimy, R., Schlezinger, D., & Eichner, E. (2006). *Linked watershed-embayment model to determine critical nitrogen loading thresholds for West Falmouth Harbor, Falmouth, Massachusetts*. Boston, MA: Massachusetts Estuaries Project, Massachusetts Department of Environmental Protection.
- Howes, B. L., Ruthven, H. E., Ramsey, J. S., Samimy, R. I., Schlezinger, D. R., & Eichner, E. (2015). *Linked watershed-embayment model to determine critical nitrogen loading thresholds for the new bedford inner harbor embayment system, New Bedford, MA (Updated Final Report)*, S Mast/DEP Massachusetts Estuaries Project. Boston, MA: Massachusetts Department of Environmental Protection.
- Howes, B. L., Samimy, R. I., Eichner, E. M., Kelley, S. W., Ramsey, J. S., & Schlezinger, D. R. (2014). *Linked watershed-embayment model to determine critical nitrogen loading thresholds for the Wareham River, Broad Marsh and Mark's Cove Embayment System, Wareham, Massachusetts*, S Mast/DEP Massachusetts Estuaries Project. Boston, MA: Massachusetts Department of Environmental Protection.
- Kroeker, K. J., Kordas, R. L., Crim, R., Hendriks, I. E., Ramajo, L., Singh, G. S., et al. (2013). Impacts of ocean acidification on marine organisms: quantifying sensitivities and interaction with warming. *Global Change Biology*, 19(6), 1884–1896. <https://doi.org/10.1111/gcb.12179>
- Kroeker, K. J., Sandford, E., Jellison, B. M., & Gaylord, B. (2014). Predicting the effects of ocean acidification on predator-prey interactions: A conceptual framework based on coastal molluscs. *The Biological Bulletin*, 226(3), 211–222. <https://doi.org/10.1086/BBLv226n3p211>
- Lewis, E., & Wallace, D. W. R. (1998). Program Developed for CO₂ System Calculations, ORNL/CDIAC-105, Carbon Dioxide Inf. Anal. Cent., Oak Ridge Natl. Lab., Oak Ridge, Tenn. (38 pp.). <https://salish-sea.pnnl.gov/media/ORNL-CDIAC-105.pdf>

- Liu, Q., Charette, M. A., Breier, C. F., Henderson, P. B., McCorkle, D. C., Martin, W., & Dai, M. (2017). Carbonate system biogeochemistry in a subterranean estuary—Waquoit Bay, USA. *Geochimica et Cosmochimica Acta*, 203, 422–439. <https://doi.org/10.1016/j.gca.2017.01.041>
- Long, M. H., Rheuban, J. E., McCorkle, D. C., Burdige, D. J., & Zimmerman, R. C. (2019). Closing the oxygen mass balance in shallow coastal ecosystems. *Limnology and Oceanography*, 64(6), 2694–2708. <https://doi.org/10.1002/lno.11248>
- Massachusetts Department of Environmental Protection (MassDEP) (2017). *Massachusetts Year 2016 integrated list of waters: Proposed listing of the condition of Massachusetts' waters pursuant to sections 305(b), 314, and 303(d) of the Clean Water Act*, (pp. 1–357). Boston, MA: Commonwealth of Massachusetts. <https://www.mass.gov/files/documents/2017/08/zu/16ilwpllist.pdf>
- Mathis, J. T., Cooley, S. R., Lucey, N., Colt, S., Ekstrom, J., Hurst, T., et al. (2015). Ocean acidification risk assessment for Alaska's fishery sector. *Progress in Oceanography*, 136, 71–91. <https://doi.org/10.1016/j.pocean.2014.07.001>
- Merrill, N. H., Mulvaney, K. K., Martin, D. M., Chintala, M. M., Berry, W., Gleason, T. R., et al. (2018). A resilience framework for chronic exposures: Water quality and ecosystem services in coastal social-ecological systems. *Coastal Management*, 46(4), 242–258. <https://doi.org/10.1080/08920753.2018.1474066>
- Millero, F. J. (2010). Carbonate constants for estuarine waters. *Marine and Freshwater Research*, 61(2), 139–142. <https://doi.org/10.1071/MF09254>
- Nicholls, S., & Crompton, J. (2018). A comprehensive review of the evidence of the impact of surface water quality on property values. *Sustainability*, 10(2), 500. <https://doi.org/10.3390/su10020500>
- Pimenta, A., & Grear, J. (2018). *Guidelines for measuring changes in seawater pH and associated carbonate chemistry in coastal environments of the Eastern United States*. Washington, DC, EPA/600/R-17/483: US EPA Office of Research and Development.
- Rheuban, J. E., Williamson, S. C., Costa, J. E., Glover, D. M., Jakuba, R. W., McCorkle, D. C., et al. (2016). Spatial and temporal trends in summertime climate and water quality indicators in the coastal embayments of Buzzards Bay, Massachusetts. *Biogeosciences*, 13(1), 253–265. <https://doi.org/10.5194/bg-13-253-2016>
- Sakashita, M. (2016). Using the Clean Water Act to tackle ocean acidification: When carbon dioxide pollutes the oceans. *Washington Journal of Environmental Law and Policy*, 6(2), 599–611.
- Soetaert, K., Hofmann, A. F., Middleburg, J. J., Meysman, F. J. R., & Greenwood, J. (2007). The effect of biogeochemical processes on pH. *Marine Chemistry*, 105(1–2), 30–51. <https://doi.org/10.1016/j.marchem.2006.12.012>
- Tank, S. E., Striegl, R. G., McClelland, J. W., & Kokej, S. V. (2016). Multi-decadal increases in dissolved organic carbon and alkalinity flux from the Mackenzie drainage basin to the Arctic Ocean. *Environmental Research Letters*, 11(5), 054015. <https://doi.org/10.1088/1748-9326/11/5/054015>
- Uppstrom, L. R. (1974). The boron/chlorinity ratio of deep-sea water from the Pacific Ocean. *Deep Sea Research and Oceanographic Abstracts*, 21(2), 161–162. [https://doi.org/10.1016/0011-7471\(74\)90074-6](https://doi.org/10.1016/0011-7471(74)90074-6)
- van Heuven, S., Pierrot, D., Rae, J. W. B., Lewis, E., & Wallace, D. W. R. (2011). MATLAB Program Developed for CO₂ System Calculations. ORNL/CDIAC-105b. Carbon Dioxide Information Analysis Center, Oak Ridge National Laboratory, U.S. Department of Energy, Oak Ridge, Tennessee. https://doi.org/10.3334/CDIAC/otg.CO2SYS_MATLAB_v1.1
- Valiela, I., Collins, G., Kramer, J., Lajtha, K., Geist, M., Seely, B., et al. (1997). Nitrogen loading from coastal watersheds to receiving estuaries: New method and application. *Ecological Applications*, 7(2), 358–380. [https://doi.org/10.1890/1051-0761\(1997\)007\[0358:NLFCWT\]2.0.CO;2](https://doi.org/10.1890/1051-0761(1997)007[0358:NLFCWT]2.0.CO;2)
- Valiela, I., Owens, C., Elmstrom, E., & Lloret, J. (2016). Eutrophication of Cape Cod estuaries: Effect of decadal changes in global-driven atmospheric and local-scale wastewater nutrient loads. *Marine Pollution Bulletin*, 110(1), 309–315. <https://doi.org/10.1016/j.marpolbul.2016.06.047>
- Waldbusser, G. G., & Salisbury, J. E. (2014). Ocean acidification in the coastal zone from an organism's perspective: Multiple system parameters, frequency domains, and habitats. *Annual Review of Marine Science*, 6(1), 221–247. <https://doi.org/10.1146/annurev-marine-121211-172238>
- Wallace, R. B., Baumann, H., Grear, J. S., Aller, R. C., & Gobler, C. J. (2014). Coastal ocean acidification: The other eutrophication problem. *Estuarine, Coastal and Shelf Science*, 148, 1–13. <https://doi.org/10.1016/j.ecss.2014.05.027>
- Wang, Z. A., Lawson, G. L., Pilskaln, C. H., & Maas, A. E. (2017). Seasonal controls of aragonite saturation states in the Gulf of Maine. *Journal of Geophysical Research: Oceans*, 122, 372–389. <https://doi.org/10.1002/2016JC012373>
- Wang, Z. A., Wanninkhof, R., Cai, W. J., Byrne, R. H., Hu, X., Peng, T. H., & Huang, W. J. (2013). The marine inorganic carbon system along the Gulf of Mexico and Atlantic coasts of the United States: Insights from a transregional coastal carbon study. *Limnology and Oceanography*, 58(1), 325–342. <https://doi.org/10.4319/lno.2013.58.1.0325>
- Wanninkhof, R., Barbero, L., Byrne, R., Cai, W. J., Huang, W. J., Zhang, J. Z., et al. (2015). Ocean acidification along the Gulf Coast and East Coast of the USA. *Continental Shelf Research*, 98, 54–71. <https://doi.org/10.1016/j.csr.2015.02.008>
- Williams, T. & Neill, C. (2014). *Buzzards Bay Coalition Citizens' Water Quality Monitoring Program, "Baywatchers", 5 Year Quality Assurance Project Plan*. New Bedford, MA.
- Williamson, S. C., Rheuban, J. E., Costa, J. E., Glover, D. M., & Doney, S. C. (2017). Changing ecosystem response to nitrogen load into the coastal estuaries within the Buzzards Bay, MA watershed. *Frontiers in Marine Science*, 3, 279. <https://doi.org/10.3389/fmars.2016.00279>
- Xu, Y. Y., Cai, W. J., Gao, Y., Wanninkhof, R., Salisbury, J., Chen, B., et al. (2017). Short-term variability of aragonite saturation state in the central Mid-Atlantic Bight. *Journal of Geophysical Research: Oceans*, 122, 4274–4290. <https://doi.org/10.1002/2017JC012901>